J. Fluid Mech. (1982), *vol.* 121, *pp.* 141–161
Printed in Great Britain

The premixed flame in uniform straining flow

By P. A. DURBIN

NASA Lewis Research Center,
21000 Brookpark Road, Cleveland, Ohio 44135, U.S.A.

(Received 28 April 1981 and in revised form 6 January 1982)

Characteristics of the premixed flame in uniform straining flow are investigated by the technique of activation-energy asymptotics. An inverse method is used, which avoids some of the restrictions of previous analyses. It is shown that this method recovers known results for adiabatic flames. New results for flames with heat loss are obtained, and it is shown that, in the presence of finite heat loss, straining can extinguish flames. A stability analysis shows that straining can suppress the cellular instability of flames with Lewis number less than unity. Strain can produce instability of flames with Lewis number greater than unity. A comparison shows quite good agreement between theoretical deductions and experimental observations of Ishizuka, Miyasaka & Law (1981).

1. Introduction

Recent interest in efficient and clean combustion has led to increasing use of controlled combustion processes (Weinberg 1974). Direct control can be achieved if fuel and oxidizer are premixed prior to combustion. Future development of premixed combustors will be aided by improved understanding of the characteristics of premixed flames, especially flames stabilized (i.e. equilibrated) in fluid flows.

Flames often are stabilized in the wake of vortex-shedding bluff bodies, and are embedded in turbulent flow. For these reasons, it is important to study the effects of flow gradients on combustion and on the stability of flames. The present paper investigates the effects of uniform straining on a steady (laminar) flame. The relevance of such analysis to flames in turbulence has been discussed by Klimov (1963) and by Clavin & Williams (1979); its relevance to flames stabilized in front of bluff bodies is described by Buckmaster (1979). Flames in combustors that might be used in jet engines are equilibrated in straining flow, and their flashback appears, in some circumstances, to be connected with an instability of the flame (Keller *et al.* 1981).

Here, activation-energy asymptotics will be used to address the problems of locating the steady flame and examining its stability. Activation-energy asymptotics are expounded in Ludford (1977*a*, *b*). Essentially, the flame is treated as an interface within which reactants are consumed and heat is released. Reactants are convected, and diffuse, toward the interface, and heat liberated by combustion is transported away from it. The combustion processes appear as discontinuities in heat and reactant fluxes across the flame; jump conditions for this discontinuity are derived through asymptotic analysis of the combustion processes occurring within the interface.

The thin-flame model, formalized by activation-energy asymptotics, was first applied to premixed flames in straining flow by Klimov (1963). A more recent analysis

by Buckmaster (1979) extends considerably the work of Klimov. Sivashinsky (1976) applied a general thin-flame equation to flames in straining flow. His model ignores the effect of straining on the structure of the pre-heat zone; however, the model shows some qualitatively correct behaviour.

When considering mixtures with Lewis number L different from unity, or flames with heat loss, two methods of analysis can be distinguished: the *direct* approach, used by Buckmaster (1979), and the *inverse* approach, used here. In the direct approach, upstream conditions are prescribed and flame properties are calculated. In the inverse approach, prescription of one of the upstream conditions is replaced by prescription of the flame temperature.

It is advantageous, when doing activation-energy asymptotics, to scale temperatures on the flame temperature. However, for prescribed upstream temperature and fuel concentration, this flame temperature is unknown *a priori* – unless the Lewis number is unity and there is no heat loss. Therefore, in the *direct* approach one has to resort to scaling on the $L = 1$, adiabatic flame temperature. As might be expected, scaling on this temperature produces non-uniformity in the asymptotic analysis, which is therefore restricted to L asymptotically near to unity, and to asymptotically small heat losses: this scaling also complicates the analysis.

If, instead of prescribing upstream conditions only, one prescribes upstream temperature and flame temperature, letting the upstream fuel concentration be determined by the analysis, it becomes possible to scale the asymptotics correctly. The solution to this *inverse* problem (i.e. find the fuel supply required to achieve a given flame temperature) can be rescaled to obtain a solution to the direct problem. We will show that, by rescaling the solution to the inverse problem, Buckmaster's results for adiabatic flames are recovered, without restrictions on L. Further, we will extend previous, adiabatic analyses by allowing downstream heat loss.

It was shown by Sivashinsky (1976) and by Buckmaster (1979) that flames can be extinguished by straining if L is sufficiently greater than unity. It will be shown here that straining can extinguish flames more effectively when there is a finite amount of heat loss. (The extinction of *diffusion* flames by straining was described by Liñan (1974).)

Our consideration of the stability of planar flames in straining flow shows that with $L < 1$ straining has a stabilizing effect. In the absence of straining, instability occurs first at very long wavelengths and leads to cellular forms (Sivashinsky 1977). Straining eliminates this long-wave instability.

In uniform flow, gaseous flames with $L > 1$ are stable in the diffusional–thermal sense, and will not become cellular. (Sivashinsky (1977) found an oscillatory, non-cellular instability for $L > 1$, but concluded that it could not appear in typical gaseous flames.) However, in flow with a large enough rate of strain, a long-wave instability of these flames appears. This instability could lead to increased flame temperature, or to extinction of the flame.

Recently, the suppression by straining of cellular instability of flames with $L < 1$ was shown experimentally by Ishizuka, Miyasaka & Law (1981). They also studied extinction and heat-loss effects on flames in straining flow. Some theoretical support for their experimental findings was offered by Law and Sivashinsky (unpublished note). The present study was done independently of that by Law and co-workers, but there are striking coincidences between the two. The present findings will be compared to observations of Ishizuka *et al.*

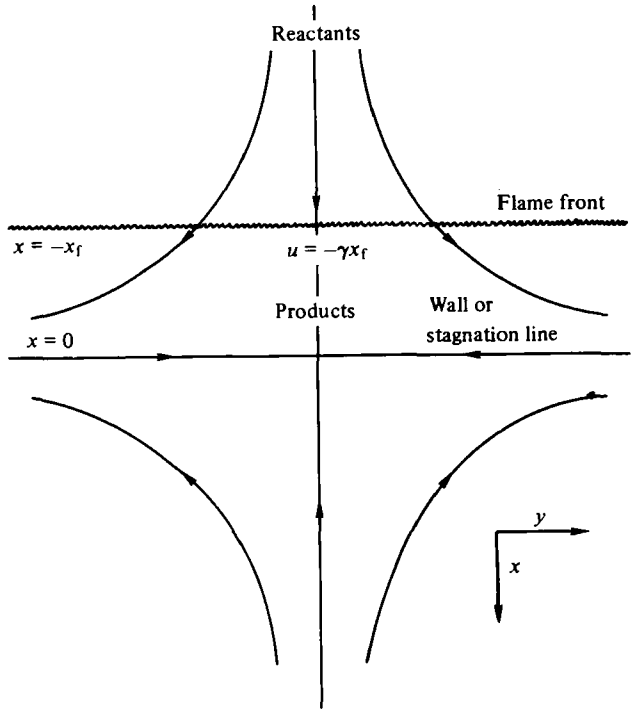

FIGURE 1. Illustration of straining flow with flame at $x = -x_f$.

In this paper we will use the constant-density, constant-property approximation. Williams (1975) notes that realistic property variations can be included in the steady-flame analysis through a suitable co-ordinate transformation. To do this conveniently, however, might require ignoring flame-generated vorticity.

The constant-density approximation *is* crucial to the present stability analysis; admission of density perturbations would severely complicate the stability equation. However, physical considerations suggest that allowing density perturbations would not qualitatively alter our deductions. Indeed, the good agreement between our analysis and the experiments by Ishizuka *et al.* is an indication that much of the relevant physics has been retained.

2. Analysis of the steady flame

The fundamental problem of steady-state flame theory is to locate the equilibrium position of a flame front in a mean flow; incorporating heat loss to surfaces where relevant. This problem can be formulated as a quite intricate free-boundary problem (Buckmaster 1979). Here we consider the simplest form of that problem; the flame is stabilized in a uniform straining flow. One knows, *a priori*, that the flame will be parallel to the axis of strain and perpendicular to the axis of compression; this is illustrated in figure 1. In the body of this paper the flow is taken to be planar. Appendix A treats the axisymmetric case.

Consider the combustion reaction to be

$$Y_1 + Y_2 \rightarrow \text{products}, \tag{1}$$

with Y_i being fuel and oxidizer. If far upstream of the flame $Y_1 - Y_2 = D > 0$, and Y_1 and Y_2 have equal diffusivity, then $Y_1 = Y_2 + D$ everywhere. One, therefore, needs only to follow the single reactant variable Y_2 as it is transported to, and consumed within, the flame.

We now pose the *inverse* problem: given the flame temperature T_*, the upstream temperature $T_{-\infty}$, and the downstream temperature T_∞, determine the flame position and fuel supply concentration as functions of straining rate. Let the straining rate be γ, Q and C_p be the heat of combustion and heat capacity of flame gases, κ and λ be the thermal and species diffusivities, and u_{L} be the usual laminar flame speed (which will be described later), evaluated at the flame temperature. Our analysis will be done for the non-dimensional quantities

$$\left.\begin{aligned} &\theta = \frac{T - T_{-\infty}}{T_* - T_{-\infty}}, \quad \theta_\infty = \frac{T_\infty - T_{-\infty}}{T_* - T_{-\infty}}, \quad Y = \frac{Y_2 Q}{C_p(T_* - T_{-\infty})}, \\ &\mathbf{x} = \tilde{\mathbf{x}} u_{\mathrm{L}}/\kappa, \quad t = \tilde{t} u_{\mathrm{L}}^2/\kappa, \quad \phi = \kappa\gamma/2u_{\mathrm{L}}^2, \\ &L = \kappa/\lambda, \quad \Delta = \frac{DQ}{C_p(T_* - T_{-\infty})}. \end{aligned}\right\} \tag{2}$$

Here tildes indicate dimensional variables. Because T_* has been used in this non-dimensionalization, we will not have to make the common restrictions that L and θ_∞ be (asymptotically) near to unity.

Consistent with the thin-flame assumption, outside the thin reaction zone the thermal and species convection–diffusion equations are

$$\left.\begin{aligned} &\partial\theta/\partial t + 2\phi y\,\partial\theta/\partial y - 2\phi x\,\partial\theta/\partial x - \nabla^2\theta = 0, \\ &\partial Y/\partial t + 2\phi y\,\partial Y/\partial y - 2\phi x\,\partial Y/\partial x - \frac{1}{L}\nabla^2 Y = 0 \end{aligned}\right\} \tag{3}$$

for the straining flow, $U = -2\phi x$, $V = 2\phi y$ of figure 1. L is the Lewis number defined in (2). Figure 1 shows two ways in which a uniform straining flow can be established: the flow can either stagnate at a wall, or it can be formed by the intersection of two counter-flowing streams. For preciseness, the latter case will be considered here.

For a steady flame, perpendicular to the x-axis, the first two terms of (3) vanish; θ and Y are then functions of x only. The boundary conditions in this case are $\theta \to 0$ as $x \to -\infty$, $\theta = 1$ at $x = -x_{\mathrm{f}}$, $\theta \to \theta_\infty$ as $x \to \infty$, and $Y \to 0$ as $x \uparrow -x_{\mathrm{f}}$; the last condition ensures that the combustion is complete to lowest order. The flame position $-x_{\mathrm{f}}$ is to be determined, as is the supply condition $Y_{-\infty}$. These quantities must be chosen such that certain jump conditions across the flame front, which will be derived next, are satisfied.

Jump conditions

This derivation of jump conditions uses the method of activation-energy asymptotics, and closely follows Ludford (1977*b*, § 4). Rather lengthy and formal derivations are available (e.g. Matkowsky & Sivashinsky 1979); we will be brief and informal.

The flame front is a plane of heat release and reactant consumption. Hence, one expects the derivatives of θ and Y to be discontinuous there, while θ and Y themselves are continuous. Denoting by [ ] the jump in the bracketed term at $-x_{\mathrm{f}}$, we have, immediately,

$$[\theta] = [Y] = 0. \tag{4}$$

Now, if the activation temperature T_a (= activation energy/gas constant) is large, the region of combustion is thin; our use of jump conditions to represent the flame is valid as $T_a \to \infty$. The dimensionless parameter $\delta \equiv T_*^2/T_a(T_* - T_{-\infty})$ is the usual small parameter of activation-energy asymptotics; it ranges typically between 0·05 and 0·1. Introducing the independent variable $\eta = (x + x_f)/\delta$ enables one to look inside the thin flame, with a view to finding the net rate of heat release; which then determines the jump in temperature and concentration derivatives.

On examination, it becomes clear that within the flame the processes of heat release by combustion, and molecular conduction of heat from the flame are in balance; because of steep gradients of θ and Y, conduction and diffusion dominate convection within the flame zone. Explicitly, if the dependent variables

$$\delta\tau(\eta) = \theta - 1, \quad \delta\chi(\eta) = Y,$$

are introduced, this balance can be written

$$Ld^2\tau/d\eta^2 = -\tfrac{1}{2}\chi(\Delta + \delta\chi)\, e^{\tau}/(\Delta + 2\delta L), \tag{5a}$$

$$d^2\chi/d\eta^2 = \tfrac{1}{2}\chi(\Delta + \delta\chi)\, e^{\tau}/(\Delta + 2\delta L), \tag{5b}$$

where the right-hand sides are the Arrhenius expressions for reaction rate, evaluated in the limit $\delta \to 0$ (Ludford 1977*a*, *b*). The factor $\chi(\Delta + \delta\chi)$ corresponds to the term $Y_1 Y_2$ that appears in the rate expression for bi-molecular reactions (see (1)). The factor e^{τ} shows the exponential dependence of reaction rate on temperature. It is because of the latter that the flame region is truly thin.

Equations (5*a*, *b*) are analogous to Ludford's (1977*b*) equation (12*a*), into which the laminar flame speed

$$u_L^2 = 2D(T_*)\,(L\delta^2(\Delta + 2\delta L)\, C_p(T_* - T_{-\infty})/Q)\, e^{-T_a/T_*} \tag{6}$$

has been inserted. $D(T_*)$ is the Damköhler number (Ludford 1977*a*, equation (4.6)). It may be thought of either as the ratio of reaction rate to thermal diffusion rate, or as the non-dimensionalized product of thermal diffusivity and squared ambient pressure.

If the solution to (5) is to match asymptotically to the steady solution to (3) we must have

$$\left.\begin{aligned} \lim_{\eta \to \infty} d\tau/d\eta, d\chi/d\eta &= \lim_{x \downarrow -x_f} d\theta/dx, dY/dx; \\ \lim_{n \to -\infty} d\tau/d\eta, d\chi/d\eta &= \lim_{x \uparrow -x_f} d\theta/dx, dY/dx. \end{aligned}\right\} \tag{7}$$

Thus an evaluation of $[d\tau/d\eta]$ and $[d\chi/d\eta]$ is equivalent to an evaluation of $[d\theta/dx]$ and $[dY/dx]$; it provides the jump conditions being sought for Y and θ.

Adding (5*a*) and (5*b*) shows that $L\tau + \chi$ must be of the form $a\eta + b$. The necessity that the reaction-zone solution match with the upstream preheat-zone solution requires $b = 0$. The matching conditions (7) determine a. Introducing the notations

$$s_+ = \lim_{x \downarrow -x_f} d\theta/dx, \quad s_- = \lim_{x \uparrow -x_f} d\theta/dx,$$

we find

$$\tau + \chi/L = s_+ \eta. \tag{8}$$

Eliminating χ between (5a) and (8) gives

$$\frac{d^2\tau}{d\eta^2} = \tfrac{1}{2}(\tau - s_+\eta)\frac{\Delta - \delta L(\tau - s_+\eta)}{\Delta + 2\delta L}e^{\tau}. \tag{9}$$

The boundary conditions for (9) are obtained by matching with the outer solution (see (7)). They are

$$\frac{d\tau}{d\eta} \to s_+ + o(\delta) \quad (\eta \to \infty), \quad \tau \to s_-\eta + o(\delta) \quad (\eta \to -\infty). \tag{10}$$

It will become clear below that satisfaction of (10) is possible only for certain values of x_f. Thus x_f is an eigenvalue for the problem (9) and (10).

The solution to (9) will be obtained for two cases: the adiabatic flame, with $s_+ = 0$, and the unimolecular reaction, with $\Delta \gg \delta$. Before considering these cases, we discuss the outer, preheat-zone solution, in order to find expressions for s_+ and s_-.

Preheat-zone solution

The preheat zone is that region, in front of and at the back of the flame, across which the temperature rises to its value at the flame. For the y- and t-independent, steady flame presently being considered, this region is governed by the following simplification of (3):

$$\left.\begin{aligned} 2\phi x\, d\theta/dx + d^2\theta/dx^2 &= 0, \\ 2L\phi x\, dY/dx + d^2Y/dx^2 &= 0. \end{aligned}\right\} \tag{11}$$

A solution to (11) satisfying (4) and the boundary conditions at $|x| = \infty$ and at $x = -x_f$ is

$$\left.\begin{aligned} \theta &= \operatorname{erfc}(-\phi^{\frac{1}{2}}x)/\operatorname{erfc}(\phi^{\frac{1}{2}}x_f) \\ Y &= -Y_{-\infty}[\operatorname{erf}((L\phi)^{\frac{1}{2}}x) + \operatorname{erf}((L\phi)^{\frac{1}{2}}x^{\frac{1}{2}})]/\operatorname{erfc}((L\phi)^{\frac{1}{2}}x_f) \end{aligned}\right\} \quad (x < -x_f), \tag{12a}$$

$$\left.\begin{aligned} \theta &= \theta_\infty + (1-\theta_\infty)\operatorname{erfc}(\phi^{\frac{1}{2}}x)/\operatorname{erfc}(-\phi^{\frac{1}{2}}x_f) \\ Y &= 0 \end{aligned}\right\} \quad (x > -x_f). \tag{12b}$$

From the solution for θ we determine

$$\left.\begin{aligned} s_+ &= 2(\theta_\infty - 1)(\phi/\pi)^{\frac{1}{2}}e^{-\phi x_f^2}/\operatorname{erfc}(-\phi^{\frac{1}{2}}x_f), \\ s_- &= 2(\phi/\pi)^{\frac{1}{2}}e^{-\phi x_f^2}/\operatorname{erfc}(\phi^{\frac{1}{2}}x_f). \end{aligned}\right\} \tag{13}$$

Equation (13) provides explicitly the boundary conditions (10). For fixed rate of strain ϕ and downstream temperature θ_∞, both s_+ and s_- are determined by x_f. It is for this reason that (9) and (10) have a solution only for certain values of x_f; if, indeed, they have a solution at all.

After the eigenvalue problem (9), (10), (13) has been solved for the flame position, the supply concentration can be found directly from (7) and (8). Thus, differentiating (8) with respect to η, letting $\eta \to -\infty$, using (7), and inserting (12a),

$$L(s_- - s_+) = \frac{2Y_{-\infty}(L\phi/\pi)^{\frac{1}{2}}e^{-L\phi x_f^2}}{\operatorname{erfc}((L\phi)^{\frac{1}{2}}x_f)}. \tag{14a}$$

Now, the usual (i.e. in the absence of straining flow) adiabatic flame temperature is just $T_{-\infty} + Y_{-\infty}(T_* - T_{-\infty})$, recalling the present non-dimensionalization (2). If this temperature is denoted by T_0, (14a) can be rearranged to read

$$\frac{T_0 - T_{-\infty}}{T_* - T_{-\infty}} = \tfrac{1}{2}L(s_- - s_+)\left(\frac{\pi}{L\phi}\right)^{\frac{1}{2}}e^{L\phi x_f^2}\operatorname{erfc}((L\phi)^{\frac{1}{2}}x_f). \tag{14b}$$

Equation (14a) provides the supply concentration required to maintain the given flame temperature. Equation (14b) gives the actual flame temperature T_* for given

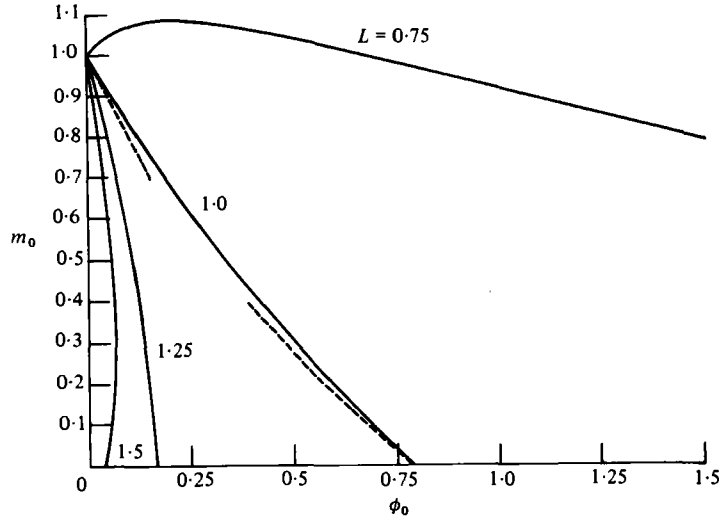

FIGURE 2. Showing flame speed *vs.* rate of strain for various Lewis numbers. The dashed lines are the asymptotes $m \to (1-2\phi)$, $\phi \to 0$ and $m \to \frac{1}{4}\pi - \phi$, $\phi \to \frac{1}{4}\pi$.

adiabatic temperature T_0. In the direct problem T_0, rather than T_*, is known. The connection (14*b*) between T_0 and T_* will be used later to obtain a solution to the direct problem by rescaling the solution to the inverse problem.

Adiabatic flame

We now proceed to integrate (9) in two special cases. In the adiabatic case $\theta_\infty = 1$; this case also might correspond to the flow towards an insulated wall in figure 1. The adiabatic flame in straining flow was considered by Klimov (1963) and by Buckmaster (1979). We include it here mainly to illustrate our inverse approach, and to show how it compares with the direct approach.

Inverse problem

When $\theta_\infty = 1$, $s_+ = 0$, and (9) becomes autonomous. We now have $\theta \equiv 1$ for $x > -x_f$, which implies that $\tau \to 0$ as $\eta \to \infty$ (see the definition of τ above (5)). Additionally, (7) requires that $\tau \to -\infty$ as $\eta \to -\infty$. Setting $s_+ = 0$ in (9), multiplying by $d\tau/d\eta$, and integrating with respect to τ between 0 and $-\infty$ gives $s_-^2 = 1$, or $s_- = 1$, or

$$(\pi/\phi)^{\frac{1}{2}} \operatorname{erfc}(\phi^{\frac{1}{2}} x_f)\, e^{\phi x_f^2} = 2. \tag{15}$$

Equation (15) determines x_f as a function of ϕ. Because the flow velocity normal to the flame at $-x_f$ is $-\gamma \tilde{x}_f$, we can define a nondimensional flame speed as $m = \gamma \tilde{x}_f / u_L = 2\phi x_f$. The relation (15) is plotted in figure 2 as m *vs.* ϕ. It is shown by the curve labelled $L = 1{\cdot}0$, with its asymptotes $m \to 1 - 2\phi$, $\phi \to 0$ and $m \to \frac{1}{4}\pi - \phi$, $\phi \to \frac{1}{4}\pi$. When ϕ becomes greater than $\frac{1}{4}\pi$ the flame speed becomes negative. Williams (1975) noted that these negative flame speeds are consistent with activation-energy asymptotics, while Buckmaster (1979) hypothesized that they are unphysical.

In an axisymmetric flame it is not possible for the flame speed to become negative with large straining; something else must happen. In appendix A we show that large rates of strain will extinguish an axisymmetric flame.

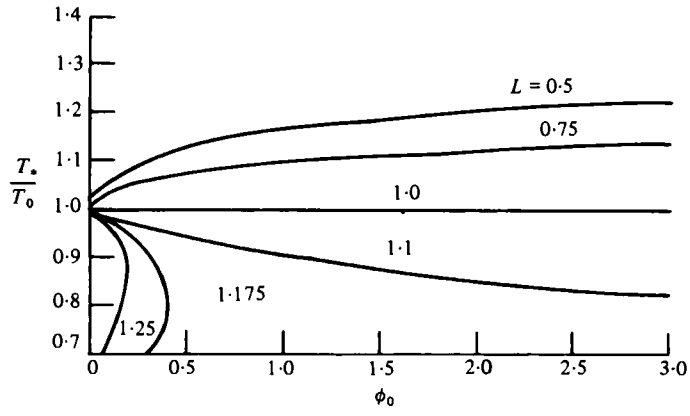

FIGURE 3. Ratio of actual to adiabatic flame temperature plotted *vs.* rate of strain, for the Lewis numbers labelling the curves.

The relation (15) is labelled $L = 1$ in figure 2 because it solves the *direct* problem when $L = 1$. It solves the inverse problem for all L (i.e. it shows flame speed *vs.* strain at *fixed flame temperature*). Where this curve is relevant, straining flow reduces flame speed – a result found previously by Klimov (1963). A combustion wave propagates by the forward diffusion of heat, through a preheat zone. The straining flow counteracts the diffusion, thinning the preheat zone and slowing the flame (Williams 1975).

Direct problem

If L is different from unity, the solutions to the inverse and direct problems differ. The solution to the direct problem is a plot of $m_0 = \gamma \tilde{x}_t / u_L^0$ *vs.* $\phi_0 = \kappa\gamma/u_L^{02}$, where u_L^0 is the flame speed (6) evaluated at the adiabatic-flame temperature T_0. The mapping $(\phi, m) \to (\phi_0, m_0)$, given by

$$(\phi_0, m_0) = ((u_L/u_L^0)^2 \phi, (u_L/u_L^0)\, m), \tag{16}$$

provides this solution to the direct problem by rescaling of the solution to the inverse problem. This rescaling can be effected because T_0 is given as a function of T_* by (14*b*).

For convenience, consider the case $T_{-\infty} \ll T_0$, T_* and $\Delta \gg \delta$. If the constant property assumption is used, then from (6)

$$(u_L/u_L^0)^2 = (T_*/T_0)^2 e^{(T_*-T_0)/(T_*\delta_0)}, \tag{17}$$

where $\delta_0 = T_0/T_a$. (The pre-exponential factor of $(T_*/T_0)^2$ in (17) is not particularly significant; the major dependence of flame speed on temperature comes through the exponential.) The solution (14*b*) for T_0/T_* determines the right-hand side of (17).

In figure 2 we have used (14*b*), (16), and (17) with $\delta_0 = 0{\cdot}1$ to plot m_0 *vs.* ϕ_0, for various L. In figure 3, T_*/T_0 is plotted *vs.* ϕ_0; this will help in understanding figure 2.

For $L < 1$, T_*/T_0 increases with straining. Therefore, so does u_L/u_L^0. Indeed, if δ_0 is small enough $m_0 = mu_L/u_L^0$ will also increase initially with straining, even though m decreases. This is shown by the curve labelled $L = 0{\cdot}75$; it agrees with Buckmaster's (1979) result that straining can increase flame speed if L is sufficiently less than unity.

When $L > 1$, T_*/T_0 decreases with straining. This decreases u_L/u_L^0, which eventually tends to zero. Thus, a given value of ϕ_0 is obtained from two values of ϕ, one small and one large (see (16)). Of course, this means that curves of m_0 *vs.* ϕ_0, and of T_*/T_0

vs. ϕ_0, must be double-valued. The curve labelled $L = 1{\cdot}5$ in figure 2, and the curves labelled $L = 1{\cdot}25$ and $1{\cdot}175$ in figure 3, are examples of double-valued functions. All curves with $L > 1$ will have a maximum ϕ_0 beyond which no solution exists. The absence of solutions at large ϕ_0 can be interpreted as extinction of the flame by large strains. This interpretation was first made by Sivashinsky (1976). Furthermore, it was shown by Buckmaster (1979) that the lower solution branch in the double-value region is unstable (however, see the present stability analysis).

Extinction can occur with m_0 greater or less than zero, depending on the value of L. It can be found numerically that with $\delta_0 = 0{\cdot}1$ extinction first occurs with $m_0 > 0$ when $L = 1{\cdot}33$; at smaller L, it occurs with $m_0 < 0$. In his asymptotic analysis, restricted to $L-1 = O(\delta_0)$, Buckmaster found that extinction with $m_0 > 0$ first occurred at $L = 1/(1-4\delta_0)$. With $\delta_0 = 0{\cdot}1$ this gives $L = 1{\cdot}67$; a value somewhat higher than the present value.

The extinction that occurs when $L > 1$ is due to a reduction in flame temperature, but not to heat loss *per se*. Straining steepens gradients of temperature and reactant, causing the heat flux out of the flame to increase more than the reactant flux into the flame. This lowers the flame temperature and leads to extinction. It turns out that downstream heat loss combined with straining is a more powerful extinction mechanism, as we shall now show.

Flame with downstream heat loss

Previous analyses of flames in straining flow have dealt only with adiabatic flames (Klimov 1963; Sivashinsky 1976; Buckmaster 1979). Heat loss is often incorporated into flame analyses by a radiative model (Buckmaster 1977; Joulin & Clavin 1979); diffusive heat loss to boundaries is modelled by a linear radiative term. In the present analysis downstream diffusive heat loss is more properly incorporated. However, one expects qualitative similarity between our results and those that would be obtained from a radiative model.

For convenience, let $\Delta \gg \delta$, so that (9) simplifies to

$$d^2\tau/d\eta^2 = \tfrac{1}{2}(\tau - s_+\eta)\, e^{\tau}. \tag{9a}$$

The solution to (9*a*), satisfying (10) with s_+ and s_- given by (13), determines x_f as a function of ϕ and θ_∞.

Because (9*a*) is non-autonomous, it can only be solved numerically. Numerical solutions to (9*a*) were obtained with a fifth-order Runge–Kutta routine, available on the NASA Lewis IBM 370/3033 computer. x_f was obtained by iteration; the iterations were done manually through the time-sharing system. The boundary conditions were applied at finite values of η, but it was checked that the limits of integration were sufficiently large to be considered infinite.

Solution to the inverse problem

In figure 4 x_f is plotted versus ϕ for various θ_∞. In figure 5 the corresponding ratio T_*/T_0, computed from (14*b*) with $T_{-\infty} = 0$, is plotted against ϕ for various θ_∞ and L. The curves for $\theta_\infty = 1$ reproduce the adiabatic results.

One observes that when $\theta_\infty < 1$ x_f becomes double-valued, and that beyond a critical strain extinction occurs (i.e. a solution for x_f ceases to exist). This is somewhat analogous to the result that, in the absence of strain, radiative heat loss causes flame

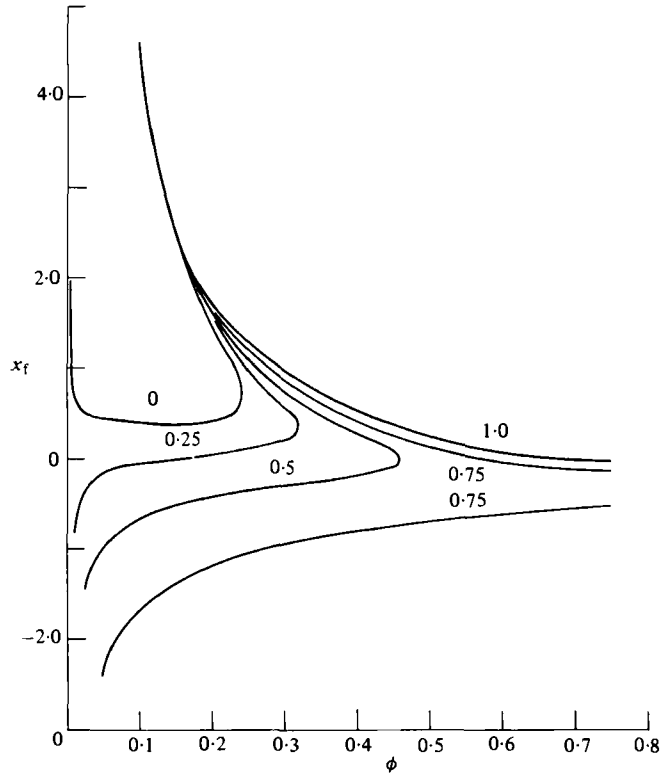

FIGURE 4. Flame position *vs.* rate of strain, with heat loss. Values of θ_∞ label the curves; $\theta_\infty = 1$ corresponds to an adiabatic flame. These curves solve the inverse problem.

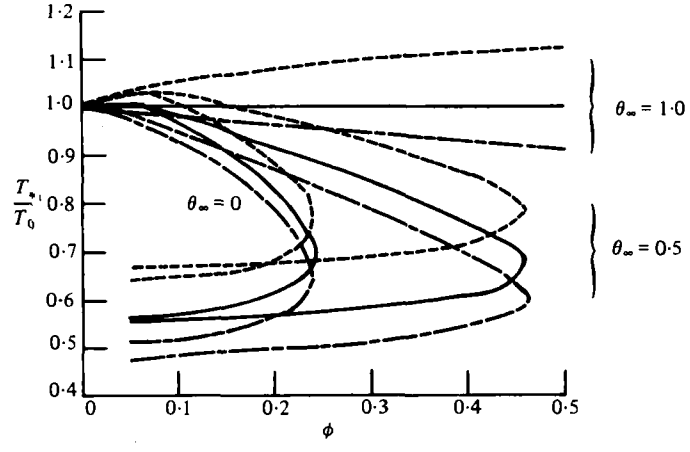

FIGURE 5. Ratio of actual to adiabatic flame temperature plotted *vs.* rate of strain. Each triplet of curves was calculated for the θ_∞ indicated. ——, $L = 1{\cdot}0$; – – –, 0·75; — — —, 1·25.

speed to become double-valued, and that beyond a critical value of heat loss extinction occurs (Buckmaster 1977). Further analysis shows that the lower branch (slower flame speed) of the double-valued solution cannot be realized because it is unstable (Spalding 1957). We have not analysed the stability of the lower solution branch in figure 4, but it seems reasonable to expect it also to be unstable.

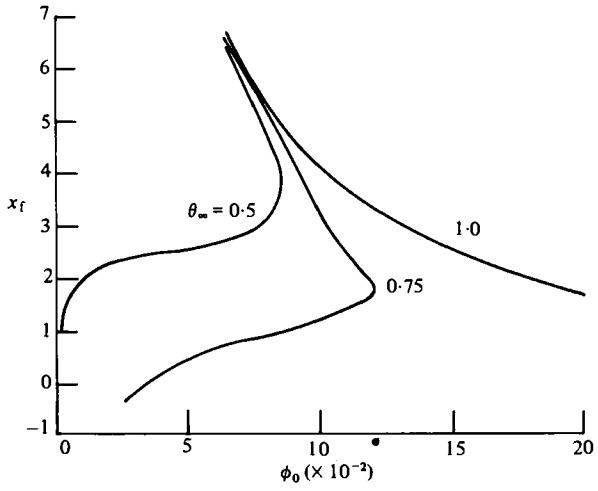

FIGURE 6. Same as figure 4, but these curves solve the direct problem for $L = 1{\cdot}0$.

Direct problem

The upper solution branch in figures 4 and 5 represents a perturbation to the adiabatic flame; the lower branch may be unphysical, as mentioned above. We will therefore consider the direct solution on the upper branch only.

Again, (16) and the temperature ratio plotted in figure 5 are used to rescale the inverse solution curve (figure 4). The result, with $L = 1$ and $\delta_0 = 0{\cdot}1$, is plotted in figure 6. As in the adiabatic case with $L > 1$, the reduction in flame temperature with straining causes the transformation of $\phi \to \phi_0$ to be two-to-one. Hence the curve of ϕ_0 versus x_f^0 has a maximum, and extinction occurs at large rates of strain. With finite heat loss, extinction can occur *at any Lewis number*. For given Lewis number, the critical strain increases, and the flame position at extinction decreases, as θ_∞ increases toward unity.

(The values of θ_∞ given in figure 5 are normalized by the *actual* flame temperature T_*. Thus their absolute value varies somewhat with strain rate. However, T_*/T_0 is not greatly different from unity on the upper solution branch, and the curves of figure 5 would not be very different were θ_∞ normalized by T_0.)

3. Stability of the flame

In this section we will consider the effect of straining flow on the stability of adiabatic flames. We realize that heat loss can have a destabilizing influence on flames (Joulin & Clavin 1979; Sivashinsky & Matkowsky 1981); however, the effect of strain is best studied, initially, by isolating its effect from that of heat loss. In his 1979 paper, Buckmaster did a preliminary analysis of stability to *one-dimensional* perturbations of flames in straining flow. Here we will consider *three-dimensional*, cellular perturbations, as these are an often-observed form of flame instability (Lewis & von Elbe 1951).

The stability of a plane flame in the absence of flow was examined by Sivashinsky (1977). He showed that the flame was unstable when $L < 1 - 2\delta$. The approach used by Sivashinsky in his analysis is quite unconventional. He adopted a co-ordinate system based on the *perturbed* flame front at the outset of his analysis. Hence his

lowest-order solution was a function of the perturbation, and was not the unperturbed state usually taken as the lowest order in stability analyses. Because of this approach, Sivashinsky's first-order problem required solution of an inhomogeneous differential equation. Sivashinsky's approach is quite correct when applied consistently; however, we will adopt a more conventional attitude, thereby avoiding the difficulties of solving inhomogeneous equations. In appendix B it is shown that in the limit $\phi \to 0$ the present stability analysis agrees with that of Sivashinsky.

We consider a perturbation to the flame front, of the form

$$\chi_f = -x_f + \epsilon\, e^{\omega t + iqz} f(ly), \tag{18a}$$

where $f(ly)$ satisfies

$$d^2f/dy^2 - 2\phi y\, df/dy = -l^2 f.$$

This, rather particular, form for $f(ly)$ is convenient and adequate for the purpose of stability analysis. The perturbation is taken to be periodic in the third dimension, z. We also let

$$\left.\begin{aligned} \Theta = \theta(x) + \epsilon\theta_0\theta'(x)\, e^{\omega t+iqz} f(ly) \quad & (x < -x_f), \\ \theta(x) + \epsilon\theta_1\theta'(x)\, e^{\omega t+iqz} f(ly) \quad & (x > -x_f), \end{aligned}\right\} \tag{18b}$$

$$\left.\begin{aligned} \Psi = Y(x) + \epsilon y_0\, Y'(x)\, e^{\omega t+iqz} f(ly) \quad & (x < -x_f), \\ 0 \quad & (x > -x_f) \end{aligned}\right\} \tag{18c}$$

be the perturbed temperature and concentration. θ and Y are the unperturbed solutions given in § 2, and the functions θ' and Y', upon which the perturbations depend, are to be determined. It will be necessary to require the perturbation amplitude to satisfy $\epsilon \ll \delta$: this requirement is perfectly justified, because only linear stability is being considered.

Modified jump conditions

The jump conditions must be reconsidered as they apply to the perturbed flame. The equations (4) are unaltered, although they must be applied at the *perturbed* flame front (18*a*). The adiabatic jump condition $[d\theta/dx] = -s_- = -1$, given above (15), is altered because $\tau(\eta)$ no longer tends to zero as η tends to infinity, as was assumed in the derivation of this condition. Indeed, matching the flame region to the preheat region now gives $\tau(\eta) \to (\epsilon/\delta)\,\theta_1 e^{\omega t+iqz} f(ly)$ as $\eta \to \infty$; where it is assumed that $\theta'(x)$ has been normalized such that $\theta'(-x_f) = 1$. As $\eta \to \infty$, χ still tends to zero. Therefore (8) is modified to

$$L\tau + \chi = L\epsilon/\delta\theta_1 e^{\omega t+iqz} f(ly). \tag{19}$$

One finds (5*a*, *b*) to be unaltered by the perturbation. Substituting (19) into (5*a*, *b*) and integrating, using the fact that τ still tends to $-\infty$ as η tends to $-\infty$, gives

$$[d\Theta/dx] = -(1 + (\epsilon/2\delta)\,\theta_1 e^{\omega t+iqz} f(ly)), \tag{20a}$$

$$[d\Psi/dx] = -L[d\Theta/dx], \tag{20b}$$

to first order in ϵ.

The present derivation of the perturbed jump conditions (20*a*, *b*) is a bit sketchy. A lengthy derivation can be found in Matkowsky & Sivashinsky (1979); the jump conditions (20*a*, *b*) correspond to their equation (60).

Stability analysis

To perform the stability analysis, we now require explicitly the functions $\theta'(x)$ and $Y'(x)$. Substituting (18*b*) into (3) gives

$$d^2\theta'/dx^2 + 2\phi x\, d\theta'/dx - (k^2+\omega)\,\theta' = 0, \tag{21}$$

where $k^2 = l^2+q^2$. We require a solution to (21) with $\theta'(-x_f) = 1$ and $\theta' \to 0$ as $|x| \to \infty$, for all ϕ. Such a solution is

$$\theta'(x) = \left.\begin{array}{ll} e^{-(\frac{1}{2}\phi x^2 - 1/4\alpha)} \dfrac{U(K+\frac{1}{2}, -(2\phi)^{\frac{1}{2}}x)}{U(K+\frac{1}{2}, \alpha^{-\frac{1}{2}})} & (x < -x_f), \\ e^{-(\frac{1}{2}\phi x^2 - 1/4\alpha)} \dfrac{U(K+\frac{1}{2}, (2\phi)^{\frac{1}{2}}x)}{U(K+\frac{1}{2}, -\alpha^{-\frac{1}{2}})} & (x > -x_f), \end{array}\right\} \tag{22}$$

where $\alpha = 1/2\phi x_f^2 = 2\phi m^{-2}$ and $K = (k^2+\omega)/\phi$. Similarly,

$$Y(x) = \left.\begin{array}{ll} e^{-L(\frac{1}{2}\phi x^2 - 1/4\alpha)} \dfrac{U(K'+\frac{1}{2}, (2L\phi)^{\frac{1}{2}}x)}{U(K'+\frac{1}{2}, (L/\alpha)^{\frac{1}{2}})} & (x < -x_f), \\ 0 & (x > -x_f), \end{array}\right\} \tag{23}$$

where $K' = (k^2+\omega L)/\phi L$. Here $U(a,b)$ are the parabolic cylinder functions defined by Abramowitz & Stegun (1965, equation (19.5.4)). Next, the constants θ_0, θ_1 and y_0 in (18) must be determined from the matching conditions. The procedure is illustrated for y_0.

To first order in ϵ, at the perturbed flame front

$$Y(\chi_f) = Y(-x_f) + \epsilon\, e^{\omega t + iqz} f(ly)\, dY/dx|_{-x_f}.$$

Thus, the condition $[\Psi] = 0$ gives

$$y_0 = 2L(\phi/\pi)^{\frac{1}{2}} e^{-\phi x_f^2}/\mathrm{erfc}\,(\phi^{\frac{1}{2}}x_f), \tag{24}$$

having used the results of § 2 to evaluate dY/dx. Similarly, $[\Theta] = 0$ gives

$$\theta_0 = \theta_1 - 2(\phi/\pi)^{\frac{1}{2}} e^{-\phi x_f^2}/\mathrm{erfc}\,(\phi^{\frac{1}{2}}x_f). \tag{25}$$

The condition (20*b*) and the solution, now known, for Ψ then gives

$$\frac{\theta_1}{2\delta m} = 2(L-p_3)(\phi/\pi)^{\frac{1}{2}} e^{-\phi x_f^2}/\mathrm{erfc}\,(\phi^{\frac{1}{2}}x_f) \tag{26}$$

again, having evaluated dY/dx at the perturbed flame front to obtain $d\Psi/dx$. In (26), and in what follows, we define

$$\left.\begin{aligned} p_3 &\equiv \frac{1}{m}\frac{dY'}{dx}\bigg|_{-x_f^-} = L(\alpha/L)^{\frac{1}{2}} \frac{U(K'-\frac{1}{2}, (L/\alpha)^{\frac{1}{2}})}{U(K'+\frac{1}{2}, (L/\alpha)^{\frac{1}{2}})}, \\ p_2 &\equiv \frac{1}{m}\frac{d\theta'}{dx}\bigg|_{-x_f^-} = \alpha^{\frac{1}{2}} \frac{U(K-\frac{1}{2}, \alpha^{-\frac{1}{2}})}{U(K+\frac{1}{2}, \alpha^{-\frac{1}{2}})}, \\ p_1 &\equiv \frac{1}{m}\frac{d\theta'}{dx}\bigg|_{-x_f^+} = -\alpha^{\frac{1}{2}} \frac{U(K-\frac{1}{2}, -\alpha^{-\frac{1}{2}})}{U(K+\frac{1}{2}, -\alpha^{-\frac{1}{2}})}, \end{aligned}\right\} \tag{27}$$

the superscripts + and − indicating $x \downarrow -x_f$ and $x \uparrow -x_f$.

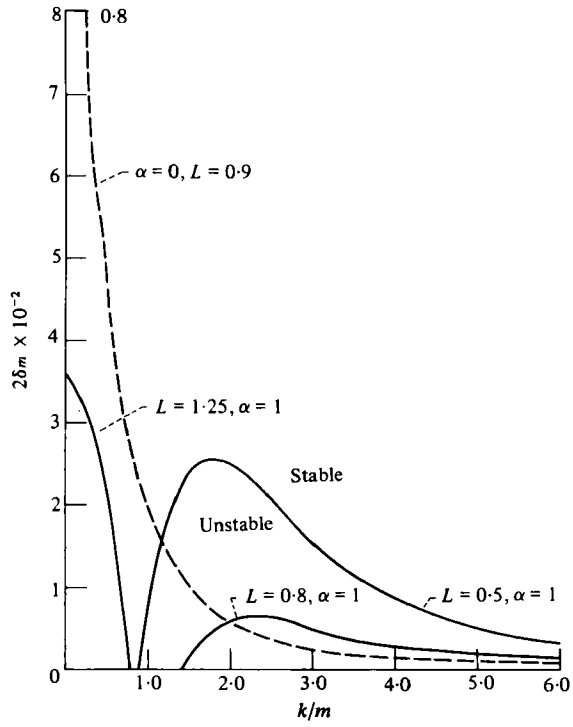

FIGURE 7. The stability boundary, $2\delta m$ *vs.* k/m, for $\alpha = 1{\cdot}0$, $L = 1{\cdot}25$, $0{\cdot}8$ and $0{\cdot}5$, and for $\alpha = 0{\cdot}0$, $L = 0{\cdot}9$.

θ_0, θ_1 and y_0 have now been determined; yet (20a) is still to be satisfied. Clearly, this condition requires a dispersion relation between k and ω to exist. In the notation of (27) this dispersion relation is

$$2\delta m = \frac{1-L+p_3-p_2}{(L-p_3)(p_1-p_2)}. \tag{28}$$

In appendix B it is shown that as $\phi \to 0$

$$\left.\begin{aligned} p_3 &\to \tfrac{1}{2}L(1+[1+4(\omega L+k^2)/L^2]^{\frac{1}{2}}\},\\ p_2 &\to \tfrac{1}{2}\{1+[1+4(\omega+k^2)]^{\frac{1}{2}}\},\\ p_1 &\to 1-p_2. \end{aligned}\right\} \tag{29}$$

Equation (28) then reduces exactly to the result of Sivashinsky (1977). (Remember that $m = 1$ when $\phi = 0$.) Sivashinsky found that, for realistic values of L and δ, instability occurred with ω real. (He found an instability with ω complex, but that occurred for values of L and δ inappropriate to most gaseous combustion.) Hence we will consider the stability boundary found by setting $\omega = 0$ in (28). One plots (28) in the form of $2\delta m$ against k, at fixed L and α, to find this neutral stability boundary. This has been done in figures 7 and 8. Figure 7 shows results for $\alpha = 1$ (corresponding to $\phi = 0{\cdot}22$) with $L > 1$ and with $L < 1$. Included for comparison is the curve for $\alpha = 0$, $L = 0{\cdot}9$: it intersects $k = 0$ at $2\delta m = 1-L = 10(\times 10^{-2})$. p_3 and p_2 are always greater than one, while the numerator of (28) is $O(10^{-2})$. Therefore, in order to calculate the curves in figures 7 and 8, p_3 and p_2 were required accurate to four decimal places. The five-decimal tables of Abramowitz & Stegun were used for these calculations.

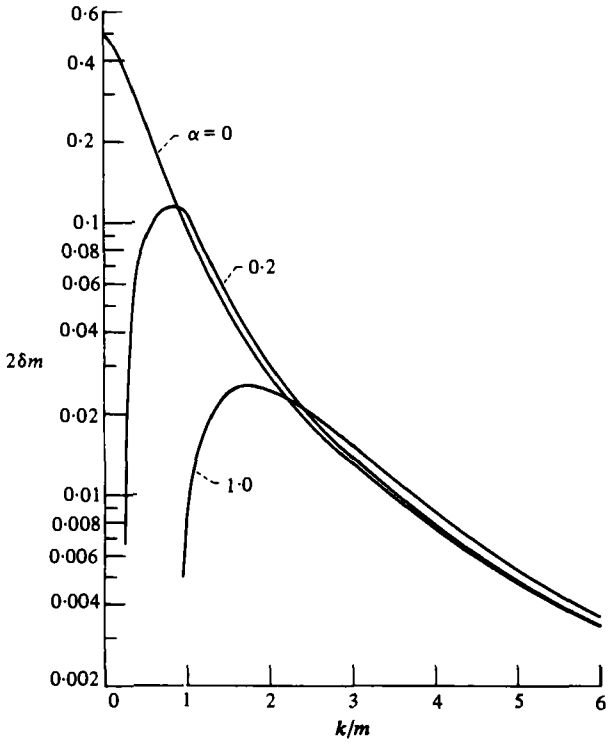

FIGURE 8. The variation of the stability boundary as α varies; $L = 0{\cdot}5$.

The right-hand side of our result (28) is zero when $L = 1$, so when $L - 1 = O(\delta)$ that equation is valid in a formal asymptotic sense. (Similarly, it is formally valid when $L > 1$ and $\alpha = O(\delta)$, or when $L < 1$ and $\alpha^{-\frac{1}{2}} = O(1/\delta)$.) However, in any real flame δ will be small but finite, and L will not be a function of δ. We have, therefore, chosen to write our dispersion relation in the form (28), and to interpret it as an *approximation* valid for small δ. Strictly speaking, then, our analysis is not based on formal asymptotics, but relies on a thin-flame model. It is fortunate, perhaps, that the right-hand side of (28) turns out to be so small. The left-hand side is assumed small in the thin-flame approximation; thus (28) could only be consistent if the right-hand side were small.

Discussion of stability results (inverse case)

It might be helpful to think of δ as a variable parameter, which determines whether or not the flame is stable. Thus, with $\alpha = 0$, and $L < 1$, the flame is stable provided δ is sufficiently large. As δ is decreased past $\frac{1}{2}(1 - L)$ long-wavelength ($k = 0$) perturbations become unstable. Further decrease of δ is accompanied by a widening band of instability, although very-short-wavelength perturbations remain stable.

Now consider the effect of strain ($\alpha \neq 0$ in figures 7 and 8). Instability still occurs when δ becomes sufficiently small, but it appears at considerably smaller values of δ than in the absence of strain, and at finite wavelength; *straining reduces the critical value of δ by suppressing the long-wave instability*. (The ordinate in the figures is $2\delta m$, but figure 2 can be used to convert this to δ.) Since δ might typically be 0·05 to 0·1, figures 2 and 7 show that moderate straining will make the premixed flame stable to

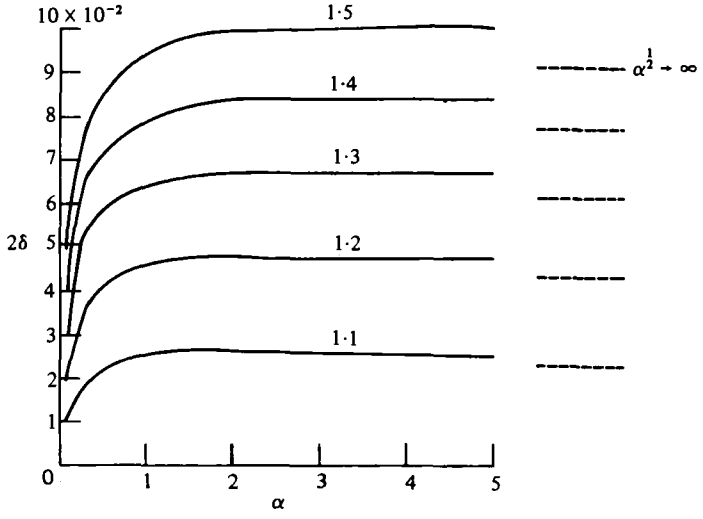

FIGURE 9. Value of 2δ at the intersection with $k = 0$ of the stability boundary, for the L indicated, *vs.* α. All L are greater than unity because this intersection is negative when L is less than unity.

perturbations. For instance, with $L = 0{\cdot}8$ instability occurs if $\delta < \frac{1}{2}(1-L) = 0{\cdot}1$ when $\alpha = 0{\cdot}0$, and if $\delta < 0{\cdot}0055$ when $\alpha = 1{\cdot}0$. Figure 8, constructed for $L = 0{\cdot}5$, shows that the flame has become stable for all δ above $0{\cdot}07$ with α as low as $0{\cdot}2$ (this α corresponds to $\phi = 0{\cdot}073$); the larger strain, $\alpha = 1{\cdot}0$ ($\phi = 0{\cdot}22$), makes the flame stable down to $\delta = 0{\cdot}02$. Note that, when $\alpha = 0{\cdot}0$ and $L = 0{\cdot}5$, instability is predicted at $\delta = 0{\cdot}25$; this value may be a bit large to be strictly consistent with activation-energy asymptotics.

A long-wave instability does still occur in the presence of finite straining, but now it appears when $L > 1$, as shown by figure 7. In figure 9 the intercept of the long-wave stability boundary with $k = 0$ has been graphed. For clarity, the stability boundary is shown here as 2δ against α, for various $L > 1$. From figure 7, one can see that this intercept of the stability boundary with $k = 0$ is the critical value of δ at which instability first occurs. As $\alpha \to 0$ the curves in figure 9 tend to $(2\delta)_{\rm cr} = 2\alpha(L-1)$; as $\alpha^{\frac{1}{2}} \to \infty$, $(2\delta)_{\rm cr} \to (L^{\frac{1}{2}}-1)/2L^{\frac{1}{2}}$.

The long-wave instability with $L > 1$ seems to correspond to the *one-dimensional* instabilities discussed by Buckmaster (1979). Buckmaster associated these with the lower solution branch of the steady flame (cf. figures 2 and 3). However, there is no unique connection between the instabilities found here and the lower solution branch. For reasonable values of δ, the instability occurs on the lower branch, but not all the branch is unstable; e.g. with $\delta_0 = 0{\cdot}1$ and $L = 1{\cdot}5$ the point ($\phi_0 = 0{\cdot}058$, $m_0 = 0{\cdot}10$) lies on the lower branch, while the corresponding $2\delta = 0{\cdot}17$ is in the *stable* region of figure 9.

In an experiment it might be difficult to reach the region of long-wave instability directly; however, by increasing fuel concentration along with strain, to maintain a constant flame temperature, one could conceivably reach this state inversely. It would be signalled, for instance, when a small increase in reactant caused a disproportionate increase in flame temperature.

Rescaling to the direct case

The individual curves of figures 7 and 8 are for given L and ϕ. Hence each curve is for a fixed value of T_*/T_0, and rescaling involves simply multiplying by an appropriate constant. Therefore, rescaling to the direct problem will not change the shapes of these curves, as did the nonlinear rescaling in § 2. Furthermore, α is non-dimensionalized by κ; i.e. it is independent of u_L. Thus (with the present constant-property approximation) α has the same value in the direct and inverse problems. The only question that arises is whether, when δ is rescaled to δ_0, strain will remain stabilizing for $L < 1$. The answer is that it will.

Because $\alpha = 2\phi m^{-2}$ is a unique function of ϕ (which can be found from the $L = 1$ curve of figure 2), the analysis of § 2 gives T_*/T_0 as a function of α. Thus the previously found critical values of δ, as a function of α, could equally have been written as $\delta_0 = \delta T_0/T_*$, as a function of α (recall our assumption that $T_{-\infty} \ll T_*$). Now $T_0 < T_*$ when $L < 1$ and $\phi > 0$, so the critical value of δ_0 is less than that of δ; *strain is even more stabilizing in the direct problem than in the inverse problem.* Corresponding to the cases cited above, and in figures 7 and 8; with $L = 0{\cdot}8$ and $\alpha = 1{\cdot}0$ $(\delta_0)_{\rm cr} = 0{\cdot}0052$, with $L = 0{\cdot}5$ and $\alpha = 0{\cdot}2$ $(\delta_0)_{\rm cr} = 0{\cdot}062$, with $L = 0{\cdot}5$ and $\alpha = 1{\cdot}0$ $(\delta_0)_{\rm cr} = 0{\cdot}017$.

Because figure 9 shows $(2\delta)_{\rm cr}$ *vs.* α, the shapes of its curves would be different if rescaled to $(2\delta_0)_{\rm cr} = T_0/T_*(2\delta)_{\rm cr}$ *vs.* α. However, because $T_0 > T_*$, when $L > 1$ $(\delta_0)_{\rm cr} > \delta_{\rm cr}$, the conclusion that straining can produce instability is unaltered.

Discussion

To conclude this section on stability, we discuss its physical mechanisms. The cellular flames, occurring when $L < 1$, are a consequence of the diffusion of reactants across corrugations of the flame front. (This has been known for some time – see Lewis & von Elbe (1951).) Reactant diffuses from unreacted regions into the higher-temperature reacted regions and, upon being consumed, increases the temperature in these regions still further; this is illustrated by figure 10(*a*). Consequently, perturbations of the flame front are amplified. Of course, this picture only holds when the reactant diffusivity is larger than the thermal diffusivity ($L < 1$). In the converse situation, heat diffuses from the reacted parts of the flame, increasing the temperature, and hence the reaction rate, in the unreacted regions. The net effect is then to cool the heated regions and heat the cool regions. The perturbation is suppressed.

These mechanisms apply when transport is solely by diffusion. In straining flow, the fluid motion transports heat and reactants at an equal rate, reducing the destabilizing effect of differential diffusion. In fact, with $k^2 + \omega = 0$ in (21) transport is solely by fluid convection; this democratic process precludes the diffusional mechanism of instability.

The long-wave instability, which occurs in straining flow with $L > 1$, does not rely on corrugations of the flame front. Instead, it is the steep gradient of Y which results in instability (figure 10*b*). When the flame position is perturbed, a large reactant perturbation occurs, *increasing*, or *decreasing*, the reaction rate in the flame. If δ is large enough the perturbed reaction rate is balanced by a perturbation of diffusive heat flux from the flame. However, if δ is small, the perturbed heat flux will not be sufficient to balance the change in heat released from reaction. Then the flame temperature rises (or falls), further increasing (or decreasing) reactant consumption. Since one

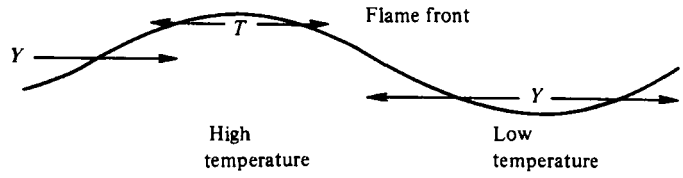

(*a*)

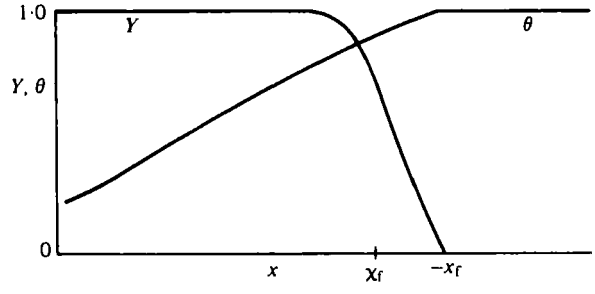

(*b*)

FIGURE 10. (*a*) Illustration of the mechanism of short-wave instability. The lengths of arrows indicate relative magnitude of diffusivities. (*b*) Exaggerated profiles of temperature and concentration for $L > 1$. The steep Y-gradient near the flame is the source of long-wave instability.

expects this mode of instability to occur on the lower branch of curves such as that with $L = 1{\cdot}25$ in figure 3 (Buckmaster 1979), a *rise* in flame temperature will stop when the upper branch has been reached. On the other hand, a *decrease* in flame temperature will lead to extinction.

The stabilizing and destabilizing effects of strain were demonstrated here by evaluating numerically the dispersion relation (28). The generality of our conclusions was not rigorously investigated, but, clearly, they hold in an experimentally realizable regime. In support of this statement, the following section compares deductions from our analysis with phenomena recently observed by Ishizuka *et al.* (1981).

4. Comparisons with experiment

Our results are in striking concord with the observations of Ishizuka *et al.* (1981). This is satisfying because our results were obtained without prior knowledge of their experimental confirmation, and because the agreement vindicates our use of the constant property approximation.

In the experiments by Ishizuka *et al.* a propane/air flame was stabilized in flow stagnating on a wall. They varied both straining rate γ and laminar flame speed u_L; the latter by adjusting propane concentration. It was found that, when ϕ was increased, either by increasing γ or by decreasing u_L, the flame moved toward the wall. As the wall temperature was increased, the flame moved away from the surface, in agreement with figure 6. Admittedly, these observations require little theoretical explanation.

Extinction away from the wall was observed experimentally at large rates of strain

(figure 6). Alternatively, at fixed rate of strain, the flame could be extinguished by decreasing fuel concentration in lean flames, or by increasing fuel concentration in rich flames; since u_L decreases away from stoichiometry, both these changes increase ϕ. By increasing the wall temperature, the extinction limits were increased, as figure 6 leads one to expect.

We suggested previously that, because $\alpha^{-1} = 2\phi x_f^2$ is non-dimensionalized by κ, it should be far less sensitive to small changes in flame temperature than quantities non-dimensionalized by u_L. Thus its value at extinction ought nearly to be independent of L and ϕ; it should depend only on rate of heat loss. Ishizuka *et al.* measured the value of α^{-1} at both lean and rich extinction for various rates of strain. At the lean limit they found that α^{-1} was indeed constant. At the rich limit, however, α^{-1} was found to increase with straining, tending asymptotically to the lean limit value. This is not explained by the present theory; Ishizuka *et al.* thought it might be due to increased heat loss at the rich limit.

A further point of agreement between theory and experiment is that in rich flames ($L < 1$) flame temperature decreased with straining. Without heat loss the opposite trend is expected; however, the maximum wall temperature which could be achieved experimentally was about $\frac{3}{4}$ of the flame temperature. Hence the curves in figure 5 with $\theta_\infty < 1$ explain the observations. Further comparisons show good agreement between experiment and the steady-flame theory described here, in Klimov (1963) and in Buckmaster (1979).

The present stability results also agree with experiment. In rich mixtures, corrugated flames were observed at small rates of strain. Upon increasing strain rate, a sharply defined transition to a smooth flame occurred. Furthermore, the strain rate at transition decreased as mixture ratio was increased (i.e. as u_L was decreased). These observations confirm our deduction that cellular instability is suppressed at a critical value of ϕ. Even the magnitude of ϕ at transition is in line with the present theory. With a mixture ratio of 1·3, transition occurred at $\gamma = 47\ \mathrm{s}^{-1}$ (figure 2 of Ishizuka *et al.* 1981). Taking $\kappa = 5\ \mathrm{cm}^2/\mathrm{s}$ (its value at 1500 °C) and $u_L^0 = 30$ cm/s (figure 218 of Lewis & von Elbe 1951) gives $\phi_0 = 0{\cdot}13$. Upon increasing the mixture ratio to 1·5, the critical value of γ decreased to 26. If the critical value of ϕ_0 is assumed to remain equal to 0·13, u_L^0 must have decreased to 22 cm/s; which is eminently reasonable.

Appendix A. Axisymmetric straining flow

In this appendix we consider an adiabatic flame with $L = 1$, in axisymmetric straining flow. For this flame the inverse and direct formulations are identical. Although the situation envisaged here might be hard to produce in its purest form, it is an approximation to a flame stabilized in the rear of a streamlined, axisymmetric body.

In axisymmetric flow, (11) becomes

$$2\phi r\frac{d\theta}{dr} + \frac{1}{r}\frac{d}{dr}\left(r\frac{d\theta}{dr}\right) = 0, \tag{A 1}$$

where the flow is from $r = \infty$ towards $r = 0$; i.e. $U_r = -\gamma r, U_z = 2\gamma z$. Because the reactants are brought from ∞ by the flow, boundary conditions to (A 1) are $\theta(\infty) = 0$,

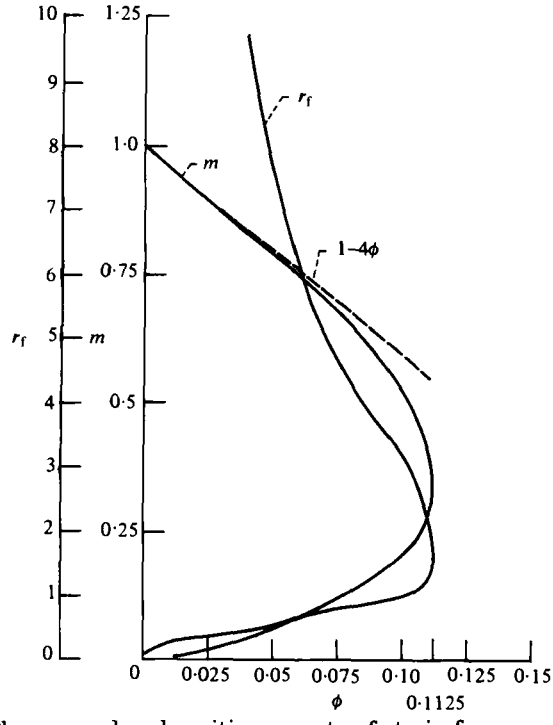

FIGURE 11. Flame speed and position *vs.* rate of strain for an axisymmetric flame. Dashed line is the asymptote $m \to 1-4\phi$, $\phi \to 0$.

$\theta(r_f) = 1$ and $[d\theta/dr] = -1$ at $r = r_f$ (assuming $r_f \gg \delta$). The appropriate solution to (A 1) is

$$\theta(r) = \begin{cases} E_1(\phi r^2)/(E_1(\phi r_f^2) & (r > r_f), \\ 1 & (r < r_f), \end{cases} \tag{A 2}$$

where E_1 is the exponential integral (Abramowitz & Stegun 1965, equation (5.1.1)). The jump condition $[d\theta/dr] = -1$ then gives

$$\tfrac{1}{2} r_f e^{\phi r_f^2} E_1(\phi r_f^2) = 1. \tag{A 3}$$

In figure 11 r_f and $m = 2\phi r_f$ are plotted versus ϕ. For given $\phi < 0{\cdot}1125$ there are two equilibrium flame positions, one with $r_f > 1{\cdot}6$ and one with $r_f < 1{\cdot}6$. There are no solutions with $\phi > 0{\cdot}1125$. Thus an axisymmetric flame can be extinguished by large strains when $L = 1$.

Appendix B. Evaluation of p_i as $\alpha \to 0$

We consider the behaviour of the p_i defined by equation (27) as $\alpha \to 0$ with $k = O(1)$. Then the parabolic cylinder functions in (27) can be approximated by applying stationary phase to their integral representations (Abramowitz & Stegun 1965, equation (19.5.4)). It is important to note that, although two points of stationary phase exist, the integration contours are such that they can be deformed to pass through only one of these points. For example

$$U(K - \tfrac{1}{2}, \alpha^{-\frac{1}{2}}) = \int_c \exp(\tfrac{1}{2}s^2 - s\alpha^{-\frac{1}{2}} - K \ln s)\, ds \tag{B 1}$$

(the contour ϵ is shown in Abramowitz & Stegun 1965, figure (19.3)) has stationary phase at

$$z_{\pm} = \tfrac{1}{2}\{1 \pm [1 + 4(k^2 + \omega)]^{\frac{1}{2}}\},$$

but only z_+ can be reached by the contour. Straightforward evaluation now shows that as $\alpha \to 0$, with k such that $k^2/\alpha \to \infty$,

$$\left.\begin{aligned} p_3 &\to \tfrac{1}{2}L\{1 + [1 + 4(k^2 + \omega L)/L^2]^{\frac{1}{2}}\}, \\ p_2 &\to \tfrac{1}{2}\{1 + [1 + 4(k^2 + \omega)]^{\frac{1}{2}}\}, \\ p_3 &\to 1 - p_2. \end{aligned}\right\} \tag{B 2}$$

REFERENCES

Abramowitz, M. & Stegun, I. A. 1965 *Handbook of Mathematical Functions*. Dover.

Buckmaster, J. 1977 Slowly varying flames. *Combust. & Flames* **28**, 225–239.

Buckmaster, J. 1979 The quenching of a deflagration wave held in front of a bluff body. In *Proc. 17th Symp. on Combustion, Pittsburgh.*

Clavin, P. & Williams, F. A. 1979 Theory of premixed-flame propagation in large-scale turbulence. *J. Fluid Mech.* **90**, 589–604.

Ishizuka, S., Miyasaka, K. & Law, C. K. 1981 Effects of heat loss, preferential diffusion and flame-stretch on flame-front instability and extinction of propane/air mixtures. Presented at Tech. Meeting Central States Section Combustion Inst., Warren, Michigan, March 1981.

Joulin, G. & Clavin, P. 1979 Linear stability analysis of nonadiabatic flames: diffusional–thermal model. *Combust. & Flame* **35**, 139–153.

Keller, J. O., Vanveld, L., Korschelt, D., Ghonium, A. F., Daily, J. W. & Oppenheim, A. K. 1981 Mechanism of instabilities in turbulent combustion leading to flashback. *Aerospace Sciences Meeting, St Louis, MO. A.I.A.A. Paper* AIAA-81-0107.

Klimov, A. M. 1963 Laminar flame in turbulent flow. *Zh. Prikl. Mekh. i Tekn. Fiz.* **3**, 49–58.

Lewis, B. & von Elbe, G. 1951 *Combustion, Flames and Explosions of Gases*. Academic.

Liñan, A. 1974 The asymptotic structure of counterflow diffusion flames for large activation energies. *Acta Astron.* **1**, 1007–1039.

Ludford, G. S. S. 1977*a* Combustion: basic equations and peculiar asymptotics. *J. Méc.* **16**, 531–551.

Ludford, G. S. S. 1977*b* The premixed flame. *J. Méc.* **16**, 553–573.

Matkowsky, B. J. & Sivashinsky, G. I. 1979 An asymptotic derivation of two models in flame theory associated with the constant density approximation. *SIAM J. Appl. Math.* **37**, 686–699.

Sivashinsky, G. I. 1976 On a distorted flame front as a hydrodynamic discontinuity. *Acta Astron.* **3**, 889–918.

Sivashinsky, G. I. 1977 Diffusional–thermal theory of cellular flames. *Combust. Sci. Tech.* **15**, 137–146.

Sivashinsky, G. I. & Matkowsky, B. J. 1981 On the stability of non-adiabatic flames. *SIAM J. Appl. Math.* **40**, 255–260.

Spalding, D. B. 1957 A theory of inflammability limit and flame quenching. *Proc. R. Soc. Lond.* A **240**, 83–100.

Weinberg, F. J. 1974 The first half-million years of combustion research and today's burning problems. In *Proc. 15th Symp. on Combustion, Tokyo.*

Williams, F. A. 1975 A review of some theoretical considerations of turbulent flame structure. *AGARD Conf. Proc.* no. 164, II1-1, II1-24.